Environmental Microbiology (2007) **9**(8), 2079–2089 doi:10.1111/j.1462-2920.2007.01324.x

Microbial control of phosphate in the nutrient-depleted North Atlantic subtropical gyre

Mikhail V. Zubkov,[1]* Isabelle Mary,[1] E. Malcolm S. Woodward,[2] Phillip E. Warwick,[1] Bernhard M. Fuchs,[3] David J. Scanlan[4] and Peter H. Burkill[1,5,6]

[1]*National Oceanography Centre, Southampton SO14 3ZH, UK.*
[2]*Plymouth Marine Laboratory, Plymouth PL1 3DH, UK.*
[3]*Max-Planck-Institute for Marine Microbiology, Bremen D-28359, Germany.*
[4]*Department of Biological Sciences, University of Warwick, Coventry CV4 7AL, UK.*
[5]*Sir Alister Hardy Foundation for Ocean Science, Plymouth PL1 2PB, UK.*
[6]*Marine Institute, University of Plymouth, Plymouth PL4 8AA, UK.*

Summary

Little is known about the dynamics of dissolved phosphate in oligotrophic areas of the world's oceans, where concentrations are typically in the nanomolar range. Here, we have budgeted phosphate uptake by the dominant microbial groups in order to assess the effect of the microbial control of this depleted nutrient in the North Atlantic gyre. Low concentrations (2.2 ± 1.2 nM) and rapid microbial uptake (2.1 ± 2.4 nM day^{-1}) of bioavailable phosphate were repeatedly determined in surface waters of the North Atlantic oligotrophic gyre during spring and autumn research cruises, using a radiotracer dilution bioassay technique. Upper estimates of the concentration of bioavailable phosphate were 7–55% of the dissolved mineral phosphate suggesting that a considerable part of the chemically measured nanomolar phosphate was in a form unavailable for direct microbial uptake. A 1:1 relationship ($r^2 = 0.96$, $P < 0.0001$) was observed between the bioavailable total phosphate uptake and the phosphate uptake of all the flow sorted bacterioplankton cells, demonstrating that bacterioplankton were the main consumers of phosphate. Within the bacterioplankton a group of heterotrophic bacteria and *Prochlorococcus* phototrophic cyanobacteria, were the two major competing groups for bioavailable phosphate. These heterotrophic bacteria had low nucleic acid content and 60% of them comprised of SAR11 clade cells based on the results of fluorescence *in situ* hybridization. Each of the two competing bacterial groups was responsible for an average of 45% of the phosphate uptake, while *Synechococcus* cyanobacteria (7%) and picoplanktonic algae (0.3%) played minor roles in direct phosphate uptake. We have demonstrated that phosphate uptake in the oligotrophic gyre is rapid and dominated by two bacterial groups rather than by algae.

Received 9 February, 2007; accepted 28 March, 2007. *For correspondence. E-mail mvz@noc.soton.ac.uk; Tel. (+44) 23 8059 6335; Fax (+44) 23 8059 6247.

Introduction

Oligotrophic oceanic gyres represent some of the Earth's largest ecosystems and profoundly affect global biogeochemistry and climate. Although it has been generally accepted that their productivity is limited by the availability of mineral nitrogen (N), recently phosphorus (P) has become implicated as another potentially limiting nutrient. Dissolved mineral phosphate concentrations fall into the low nanomolar range in oligotrophic regions of the North Pacific (Karl *et al*., 1997) and western North Atlantic (Wu *et al*., 2000) as well as in the Mediterranean Sea (Thingstad *et al*., 2005). These low phosphate concentrations have been interpreted as growth limiting or colimiting to phytoplankton species that populate these waters (Sanudo-Wilhelmy *et al*., 2001; Mills *et al*., 2004). Whether oligotrophic regions exhibit trace metal (e.g. iron Fe), P or N limitation/colimitation for phytoplankton growth has received much attention (Arrigo, 2005). However, little is known about *in situ* rates of microbial N and P cycling except that the dominant microbes found in these waters actively fix carbon (Li, 1994) and are metabolically active (Zubkov *et al*., 2004; Mary *et al*., 2006).

The numerous forms of inorganic dissolved N does not allow complete microbial budgets of this element to be determined easily (Lipschultz, 1995). Conversely, the phosphate budget of surface waters of an oligotrophic gyre is easier to quantify because inorganic P is present only in one form phosphate, albeit at low nM concentrations. In the present study, we assessed the microbial control of phosphate in the central, eastern parts of the North Atlantic oligotrophic gyre (Fig. 1) by

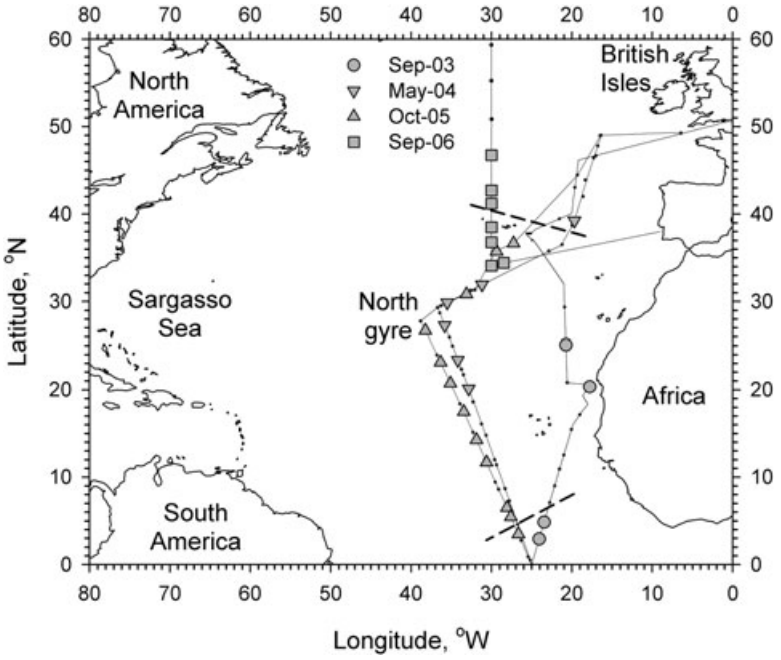

Fig. 1. Schematic presentation of the North Atlantic oligotrophic gyre studied on four meridional transect cruises. Symbols indicate stations at which uptake rates of bioavailable phosphate were determined. Solid lines with dots indicate cruise tracks and additional (non-essential) stations. Thick dashed lines indicate the boundaries of bioavailable phosphate depleted (< 6 nM) surface waters.

determining the contributions of each of the dominant microbial groups to phosphate uptake.

To overcome difficulties of quantifying nanomolar concentrations of depleted phosphate and to constrain budgeting, we used two different approaches: a nanomolar analytical chemistry method that measures the concentration of dissolved mineral phosphate in surface seawater samples and a radiotracer dilution bioassay method that estimates the maximum ambient concentration of bioavailable phosphate as well as the microbial uptake rate of bioavailable phosphate. We also compared phosphate bioavailability with the bioavailability of the dissolved organic phosphorus (DOP) pool using adenosine 5′-triphosphate tracer (^{33}P-ATP) as a model molecule. Bioavailable phosphate uptake by the dominant microbial groups was quantified using flow cytometric sorting of [^{33}P]orthophosphate labelled microorganisms. The most general and numerous group of microbes was DNA stained bacterioplankton, which was discriminated and flow sorted from other particles in the water. Low nucleic acid (LNA) containing bacterioplankton cells, which lacked autofluorescence, were flow cytometrically discriminated from other DNA stained bacterioplankton. *Prochlorococcus* (*Pro*), *Synechococcus* (*Syn*) cyanobacteria and picoplanktonic algae were initially identified by flow cytometry using chlorophyll and phycoerythrin autofluorescence. The flow sorted bacterioplankton groups were phylogenetically characterized using fluorescence *in situ* hybridization (FISH) technology. Ultimately, the approach outlined here enabled us to compare bioavailable phosphate uptake rates by phylogenetically characterized dominant bacterial groups and cells in both relative and absolute amounts.

Results and discussion

Using four research cruises (Fig. 1), we found phosphate concentrations to be depleted in the surface waters of the central, eastern parts of the North Atlantic gyre. The observed concentrations of dissolved mineral phosphate of 7.0 $\pm$ 2.9 nM, $n = 19$ (Fig. 2a) were typical for phosphate depleted marine systems (Thingstad *et al.*, 2005). Comparing measurements of these concentrations and the microbial uptake rates of bioavailable phosphate (Fig. 2), we found phosphate depletion in surface waters of the central-eastern part of the North Atlantic gyre to be a recurrent feature particularly in early autumn but possibly also in late spring (Table 1). This is in agreement with results reported for the Sargasso Sea further to the west of the North Atlantic gyre (Wu *et al.*, 2000; Ammerman *et al.*, 2003). The upper estimates of the concentration of bioavailable phosphate were 7–55% of the dissolved mineral phosphate concentrations suggesting that much of the measured mineral phosphate is in a form unavailable for direct microbial uptake.

Although the discrepancies between the mineral and bioavailable phosphate measurements require further investigation some critical comments can be made. Because of acid hydrolysis of unfiltered samples, part of the chemically measured dissolved phosphate could derive from hydrolysed DOP as well as from microbial cells. For example, the mean amount of total P in bacte-

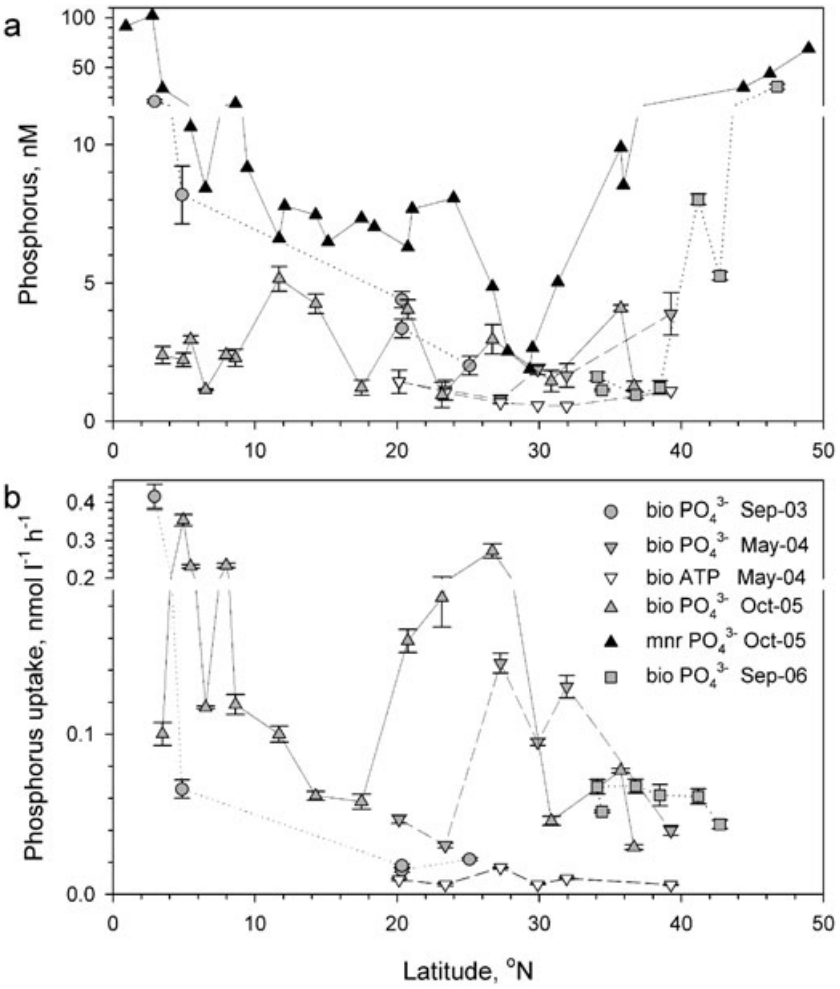

Fig. 2. Latitudinal distribution of (a) concentrations of nanomolar mineral phosphate (mnr PO_4^{3-}), bioavailable phosphate (bio PO_4^{3-}) and adenosine 5′-triphosphate (bio ATP).
b. Total uptake rates of bioavailable phosphate and ATP in surface waters of the North Atlantic gyre. The corresponding dates of cruise measurements are shown in the symbol legend, which applies to both plots. Notice the breaks in the *y*-axis.

rioplankton plus picoplanktonic algae determined using abundance and cell P content (Gundersen *et al*., 2002; Ho *et al*., 2003) was estimated to be 6.9 ± 2.9 nM. This concentration is comparable to that for the measured mineral phosphate concentration. There is also a possibility that a proportion of mineral phosphate measured could come from phosphate adsorbed to seawater colloids, and then released by acid hydrolysis. Therefore, we suggest that compared with the chemical analytical method, the bioassay method provides a more realistic estimate of dissolved phosphate concentrations. Consequently, bioavailable phosphate estimates were used for computing absolute phosphate uptake rates of the microbial groups and cells.

As well as bioavailable phosphate, DOP may also be used by microorganisms. We therefore assessed DOP bioavailability using ATP as a model compound. Despite its instability in seawater, bioassayed measurable ATP was found at concentrations of 0.90 ± 0.36 nM (Fig. 2a). Such concentrations are comparable to the bioavailable

Table 1. Comparison of bioassay estimates of maximum concentration and microbial uptake rates of bioavailable phosphate in the North Atlantic oligotrophic gyre made on the meridional transect cruises in four consecutive years.

Cruise dates	Bioavailable Phosphate phosphate (nM) Avg ± SD	uptake rate (nM day^{-1}) Avg ± SD
September 2003	3.3 ± 1.2 (3)	0.44 ± 0.08 (3)
May 2004	1.8 ± 1.1 (4)	2.0 ± 1.2 (4)
October 2005	2.4 ± 1.3 (15)	3.4 ± 2.3 (15)
September 2006	1.2 ± 0.3 (4)	1.5 ± 0.2 (4)
Average[a]	2.2 ± 1.2 (26)	2.1 ± 2.4 (26)

a. An average for all measurements made.
Numbers in brackets indicate the numbers of individual measurements.
Avg, average value for a cruise; SD, its standard deviation.

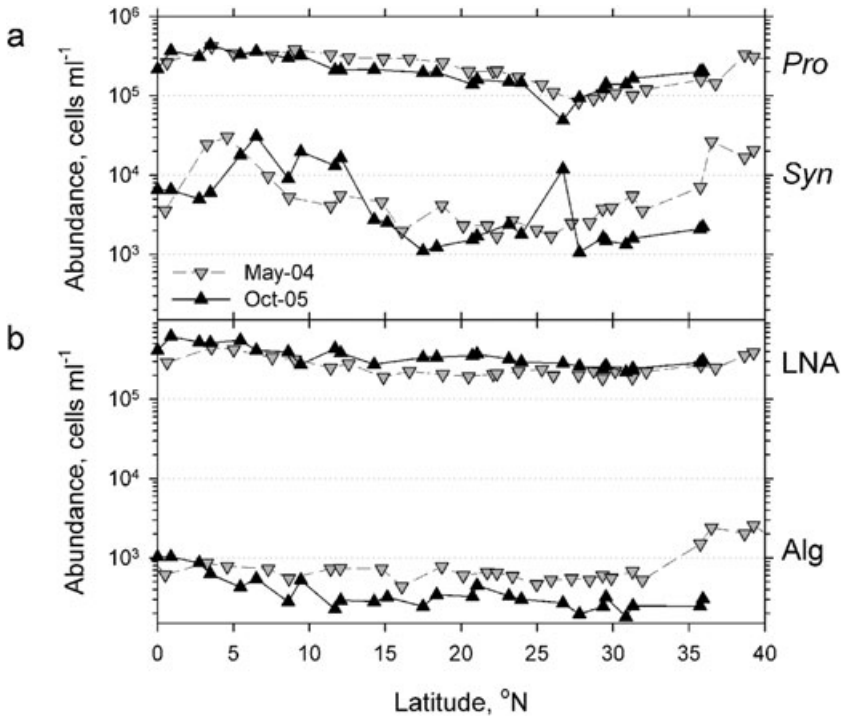

Fig. 3. Latitudinal distribution of the abundance of (a) *Prochlorococcus* (*Pro*) and *Synechococcus* (*Syn*) cyanobacteria; and (b) bacterioplankton with low nucleic acid cell content (LNA) and picoplanktonic algae (Alg) in the surface waters at stations on the May 2004 and October 2005 cruises. Notice the log scales of the *y*-axis. Dotted horizontal lines indicate the orders of magnitude to aid comparisons. The symbol legend applies to both plots.

phosphate concentrations (Table 1), but had a relatively slow uptake time of 2–15 days, and a low microbial ATP uptake rate of 0.22 ± 0.10 nM day^{-1}, $n = 6$ (which is 13 ± 6% of the phosphate uptake rate) (Fig. 2b). From this comparison, we conclude that ATP and possibly other nucleotides, are playing a secondary but not insignificant role in microbial P acquisition in the gyre ecosystem, compared with phosphate. Other pools of DOP, including phospholipids and high molecular weight DOP exist and ATP would be an inadequate model molecule for these. The bioavailability of such pools would require further study.

Prochlorococcus cyanobacteria (Fig. 3a) and LNA bacterioplankton (Fig. 3b) were the two numerically dominant groups of microorganisms enumerated by flow cytometry while *Synechococcus* cyanobacteria were the most variable group of picoplankton enumerated (Fig. 3a). *Syn* cells were about 100 times less abundant than *Pro* cells (except at one station, 26.7°N), but still 10 times more abundant than the algal cells in the centre of the gyre (15°N–30°N). The abundance of *Pro* cells in surface, phosphate deplete, waters of the North Atlantic gyre (Fig. 1) was approximately 30% higher in late spring compared with early autumn. The opposite was true for LNA cells. Their numbers were 50% higher in autumn, indicating possible minor seasonal variability. This seasonal variability was greater for the least abundant group of picoplankton, the algal cells, which were 2.5 times more numerous in late spring (Fig. 3b). However, the observed seasonal variability of picoplankton abundance seemed to have no pronounced effect on either bioavailable phosphate concentrations or microbial uptake rates of phosphate (Table 1, Fig. 2).

Phylogenetic composition of the bacterioplankton community was similar to that observed previously in surface waters of the tropical Atlantic (Mary *et al*., 2006). Bacteria, identified by FISH using the EUB I–III probe (Table 2) and visualized after DNA staining, comprised 76 ± 5% ($n = 8$) of all prokaryotic cells. These concentrations are 12% less than reported previously (Mary *et al*., 2006). The remaining 24% of prokaryotic cells were unidentifiable by FISH. This may be because some of the cells in the more oligotrophic waters of the North Atlantic gyre had an insufficient number of ribosomes for detection by that technique. However, we cannot exclude the possibility that the unidentified cells may belong to phylogenetic groups not targeted by the probes used (Table 2). For example Archaea may be present although, previous reports have suggested their low abundance in oceanic surface waters (Karner *et al*., 2001).

The SAR11 clade (Morris *et al*., 2002), represented the largest proportion (32 ± 3%) of all prokaryotic cells, while cyanobacteria (using probe Cya664, Table 2) represented 24 ± 7% of all prokaryotic cells. *Pro* (using probe 405Pro, Table 2) represented 26 ± 7% of all prokaryotic cells or virtually all identifiable cyanobacteria and *Syn* (using probe 405Syn, Table 2) represented only 0.8 ± 0.04%. The relative abundance of *Syn* in the bacterioplankton, as determined by FISH and flow cytometry, 0.7 ± 0.8%, was essentially the same. Flow cytometric and FISH enumera-

Table 2. FISH oligonucleotide probes used for phylogenetic affiliation of bacterioplankton cells.

Probe	Specificity	Sequence (5′–3′) of probe	FA[a] (%)	NaCl[b] (mM)	Reference
EUB I–III	Bacteria	GCWGCCWCCCGTAGGWGT	35	80	Amann *et al*. (1990); Daims *et al*. (1999)
SAR11–542R	SAR11 clade	TCCGAACTACGCTAGGTC	30	112	Morris *et al*. (2002)
Cya664	Cyanobacteria	GGAATTCCCTCTGCCCC	35	80	Schönhuber *et al*. (1999)
405Pro	*Prochlorococcus*	AGAGGCCTTCGTCCCTCA	40	56	West *et al*. (2001)
645LL	Low-light *Pro* group	ACCATACTCAAGCCAATC	30	112	West *et al*. (2001)
645HLI	High-light *Pro* group I	ACCATACTCAAGCCGATC	35	80	West *et al*. (2001)
645HLII	High-light *Pro* group II	ACCATACTCAAGCCTTTC	35	80	West *et al*. (2001)
405Syn	*Synechococcus*	AGAGGCCTTCATCCCTCA	40	56	West *et al*. (2001)

a. Percentage of formamide in *in situ* hybridization buffer.
b. NaCl concentration in washing buffer.

tion of *Pro* showed statistically significant 1:1 agreement (slope 0.99 ± 0.18, $r^2 = 0.83$, $P < 0.0014$, $n = 8$) confirming accurate enumeration of stained *Pro* cells with virtually undetectable low chlorophyll autofluorescence in surface waters. The sum of cyanobacterial and SAR11 percentages would be 55%, leaving 45% of all prokaryotic cells or 20% of Bacteria, which were 76% of all prokaryotic cells, unidentified with the limited set of probes used (Table 2).

The flow cytometrically sorted LNA and *Pro* groups were also phylogenetically characterized by FISH. The vast majority of cells (88 ± 3%, $n = 4$) sorted from the stained *Pro* cluster were identified as *Pro* cells (using probe 405Pro, Table 2) while a similar summed percentage of cells, 88 ± 3%, belonged to the two high-light (HL) adapted ecotypes (West *et al*., 2001). The low-light (LL) adapted ecotype was undetectable. In agreement with earlier observations (West and Scanlan, 1999; Johnson *et al*., 2006; Zwirglmaier *et al*., 2007) the composition of *Pro* differed across the North Atlantic gyre. At two stations above 30°N 53 ± 3%, $n = 2$ and 36 ± 3% of cells belonged to the HLII and HLI ecotypes, respectively, while the area below 30°N was dominated by the HLII ecotype (80 ± 1%, $n = 2$), with only 9 ± 3% of the HLI ecotype. The SAR11 clade comprised 61 ± 2%, $n = 4$ of the LNA cells in agreement with previous observations (Mary *et al*., 2006).

Flow sorting of [^{33}P]orthophosphate labelled cells demonstrated a close relationship between the measured total bioavailable phosphate uptake and the phosphate uptake of flow sorted bacterioplankton (Fig. 4a) in surface waters of the North Atlantic gyre. The two sets of values were statistically very similar, except for one outlier that showed a relatively small 16% difference. This shows bacterioplankton to be the main consumer of bioavailable phosphate. Comparison of bacterioplankton phosphate uptake with the sum of phosphate uptake of the LNA, *Pro* and *Syn* groups determined by multiplying their mean cellular phosphate uptake by the corresponding group abundance also showed a close to 1:1 agreement (Fig. 4b). Hence, the three flow-sorted bacterial groups accounted for approximately 94% of phosphate uptake of the flow-sorted bacterioplankton group. This budgeting of the total phosphate uptake by summing the rates of the flow sorted groups suggested that other unaccounted microbial groups contributed little to phosphate uptake, except for the relatively small contribution seen at the outlier (Fig. 4a).

Despite their high cell uptake rates (Fig. 5b), the *Syn* and algal groups played a minor role in phosphate uptake (Figs 4b and 5a) due to the generally very low abundance of *Syn* and algae in the gyre compared with the *Pro* and LNA groups (Fig. 3). On average, the *Syn* group accounted for 6.5 ± 3.4% of bacterioplankton phosphate uptake, and the algal group only 0.33 ± 0.19% of total phosphate uptake. The *Pro* and LNA groups intermittently dominated phosphate uptake (Fig. 4c), on average accounting for 43 ± 16% and 45 ± 26% respectively. Taking into account the estimated rapid uptake rates of phosphate (Fig. 2b), then we interpret the even scattering of points across the unity line (Fig. 4c), and the extremity of variance and similar cell uptake rates (Fig. 5b) as being an indication of competition for phosphate between the *Pro* and LNA groups.

We envisage this competition for phosphate between the two groups as being neither entirely exclusive nor entirely mutualistic. Thus, although heterotrophic LNA cells could depend on organic carbon synthesized by *Pro*, and *Pro* could depend on LNA cells for recycling of reduced N, we suggest that interactions between the two groups give rise to a more 'competitive balanced' relationship with an unstable optimum, as the broad scattering of points in Fig. 4c indicate. This unstable balancing of *Pro* and LNA groups could be explained by protist predation as our indirect experimental evidence of high amino acid accumulation by picoplanktonic protists suggests (M.V. Zubkov, unpubl. data).

Certainly, strong competitive pressure by LNA cells would explain why *Prochlorococcus* possesses diverse molecular and physiological adaptations to phosphate shortage (Moore *et al*., 2005; Martiny *et al*., 2006), one of

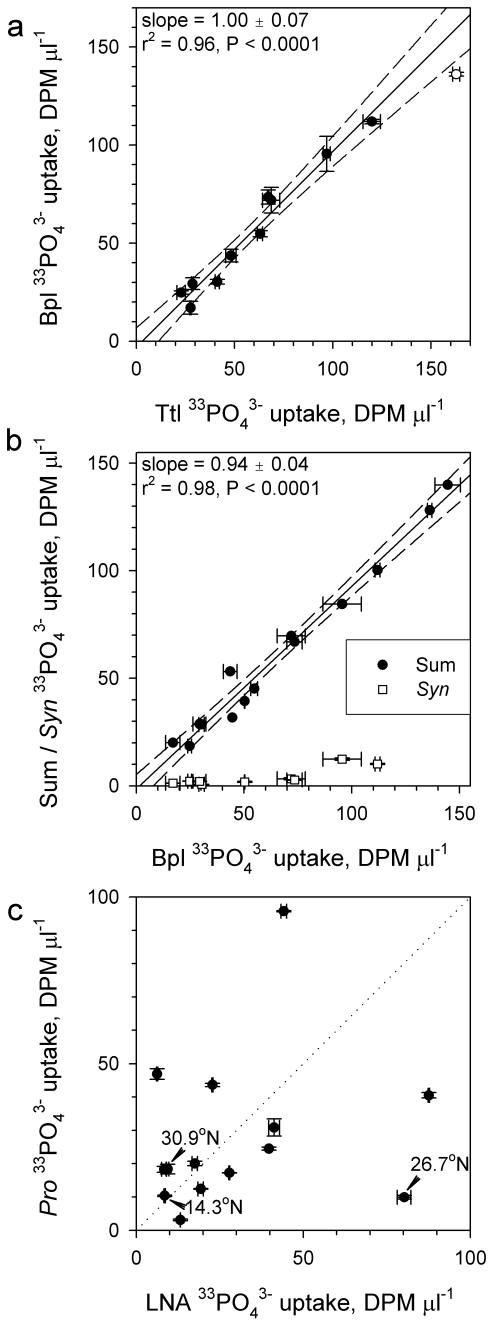

Fig. 4. Scatter plot comparisons of phosphate ($^{33}PO_4^{3-}$) uptake measured on the cruise in September 2005.
a. Total uptake rates of bioavailable phosphate (Ttl) versus uptake rates of flow-sorted bacterioplankton (Bpl).
b. The bacterioplankton phosphate uptake rates versus summed (Sum) rates of the flow sorted dominant bacterioplankton groups or *Synechococcus* (*Syn*) group rates.
c. Phosphate uptake of the LNA group versus the *Prochlorococcus* (*Pro*) group rates. Error bars indicate single standard errors of the measurements. Solid lines in (a) and (b) are linear regression lines and short dash lines indicate 95% confidence corridors. The open circle in (a) shows the outlier. Corresponding regression slopes, coefficients and statistical probabilities are presented on the plots. The dotted line in (c) is a unity line. Arrows and latitude labels indicate the measurements that are presented in more detail in Fig. 5. The symbol legend applies to plot (b) only.

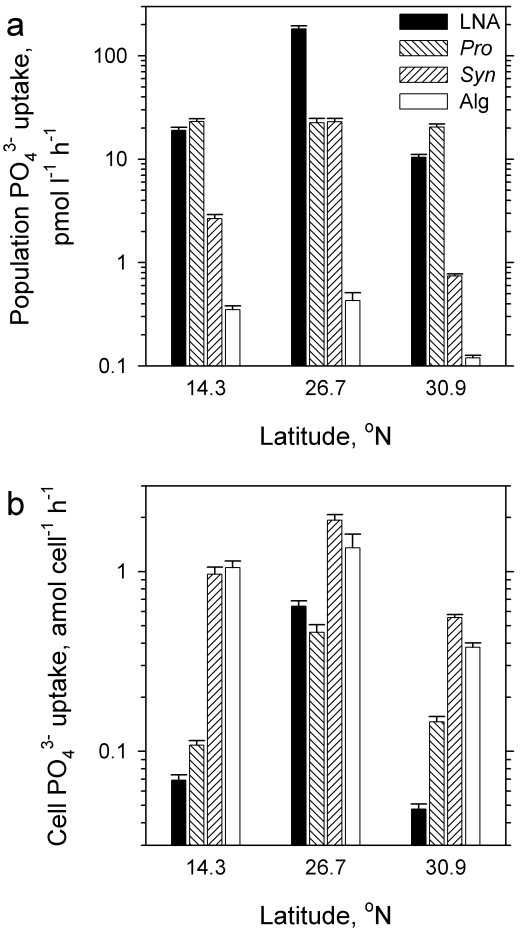

Fig. 5. Bar chart comparison of microbial uptake rates of phosphate (PO_4^{3-}) measured on the cruise in September 2005.
a. Phosphate uptake of the LNA, *Pro*, *Syn* and picoplanktonic algae (Alg) groups and (b) cells at three selected stations (Fig. 4c). Error bars indicate single standard errors. Notice the log scales of the *y*-axis. The symbol legend applies to both plots.

which is the synthesis of sulfolipids instead of phospholipids (Van Mooy *et al*., 2006). We would expect then that similar physiological and molecular adaptations exist in LNA cells, including the SAR11 clade. However, current knowledge of how LNA cells adapt to phosphate shortage is limited, although the molecular evidence for a streamlined, minimal genome is mounting for some LNA representatives, e.g. *Pelagibacter ubique* (Giovannoni *et al*., 2005). It is noteworthy although that we have not observed noticeable latitudinal changes in phosphate uptake of the *Pro* group following the observed ecotype shifts, which suggests similar phosphate uptake rates by the HLI and HLII ecotypes.

Using earlier measurements of CO_2 fixation (Li, 1994) and the present measurements of phosphate uptake by phytoplankton cells in the northern part of the North Atlantic gyre we have estimated C : P uptake ratios of phytoplankton cells to assess how realistic our absolute

phosphate uptake estimates per cell really are. The calculated C : P molar uptake ratios for *Pro* and *Syn* cells were approximately 100 and 140, respectively, close to those reported for cyanobacterial growth under P-replete conditions (Bertilsson *et al*., 2003; Heldal *et al*., 2003). This suggests that although phosphate is depleted in the northern part of the North Atlantic gyre it does not limit cyanobacterial growth to the level that would affect their cellular C : P ratio. In contrast, the C : P ratio for algae was an order of magnitude higher than a typical ratio for eukaryotic phytoplankton growth under P-replete conditions (Ho *et al*., 2003). The approximately 1000:1 C : P ratio of algal cells suggests that algae could be phosphate limited in the North Atlantic gyre. However, simultaneous measurement of phosphate acquisition and C fixation rates of the same cells are required to fully ascertain this.

Conclusion

The present study shows that bacterioplankton dominated uptake of bioavailable phosphate in surface waters of the North Atlantic gyre and suggests that there is rapid competitive uptake of depleted phosphate by the *Prochlorococcus* and LNA groups. In contrast, *Synechococcus* and picoeukaryotic phytoplankton played only a minor role in direct phosphate uptake.

Experimental procedures

Sampling and microbial enumeration

The study was carried out on board the Royal Research Ship (R.R.S.) James Clark Ross in September–October 2003 and in May 2004, on board the R.R.S. Discovery in September–October 2005, and on board the Research Vessel (R.V.) Maria S. Merian in September–October 2006. Surface seawater samples were collected from a depth of 2–7 m with a sampling rosette of 20-litre Niskin bottles mounted on a conductivity-temperature-depth (CTD) profiler at stations identified in Fig. 1. The samples were fixed with 1% paraformaldehyde (PFA) and used to enumerate microbial plankton (Fig. 3) using flow cytometry. *Syn*, *Pro* and algae were enumerated in unstained samples (Supplementary online Fig. S1) with a FACSort flow cytometer (Becton Dickinson, Oxford, UK) using their specific chlorophyll/phycoerythrin autofluorescence (Olson *et al*., 1993). Abundance of the LNA, *Pro*, in cases where chlorophyll fluorescence was below the detection limit, and total bacterioplankton (Supplementary online Fig. S2) were determined after staining with SYBR Green I DNA dye (Marie *et al*., 1997; Zubkov *et al*., 2000). Yellow-green 0.5 μm reference beads (Fluoresbrite Microparticles, Polysciences, Warrington, USA) were used in all analyses as an internal standard for both fluorescence and flow rates. The absolute concentration of beads in the stock solution was determined using syringe pump flow cytometry (Zubkov and Burkill, 2006).

Determination of dissolved mineral phosphate

Samples for nanomolar nutrient analysis were taken from the Niskin bottles on the CTD/Rosette system as described earlier. The nutrient samples were taken as soon as practicable after the CTD came on board and as early in the sampling scheme as possible using clean sampling techniques (Woodward, 1994). All bottles used were acid cleaned 'aged' HDPE type and the samples were all analysed as soon as practicable after sampling, beginning with the nearer surface samples first. The samples were not stored, preserved or frozen prior to analysis. Phosphate concentrations for the surface waters of the North Atlantic gyre were determined at nanomolar concentration levels. The analytical methodology used was taking sensitivity optimized colorimetric segmented flow analytical techniques and coupling them with 2-m Liquid Waveguide capillary cells (World Precision Instruments), a high intensity light source and photodiode detectors (Woodward, 2002). This gave detection limits of about 1–2 nmoles l^{-1}.

Bioassay of phosphate concentration and microbial uptake rates using radioactively labelled precursor

The concentrations of bioavailable phosphate and microbial uptake rates were estimated using a concentration series bioassay (Wright and Hobbie, 1966; Zubkov and Tarran, 2005) of untreated live samples, in order to avoid the uncertainties of analytical measurements associated with the separation of dissolved and particulate pools (Ferguson and Sunda, 1984). The ATP bioassays were performed on the May 2004 cruise only.

The samples used for rate determinations were initially collected into acid-washed 1-l thermos flasks using acid soaked silicone tubing and were processed within 1 h after sampling. [^{33}P]orthophosphate (> 2500 Ci $mmol^{-1}$, Amersham Biosciences UK) was added at a standard concentration of 0.02 nM and diluted with non-labelled phosphate using a dilution series of 0.4 nM, 0.8 nM, 1.6 nM, 3.2 nM and 4.8 nM [γ^{33}P]ATP (~3000 Ci $mmol^{-1}$, Amersham Biosciences UK) was added at a standard concentration of 0.02 nM and diluted with non-labelled ATP using a dilution series of 0.2 nM, 0.4 nM, 0.6 nM, 0.8 nM and 1.0 nM.

Triplicate samples (1.6 ml) for each addition were incubated in 2-ml screw top-capped sterile polypropylene microcentrifuge tubes in the dark, and at *in situ* temperatures. A sample was fixed at each of 15, 30 and 45 min or 20, 40 and 60 min, by adding PFA, to give a 1% final concentration. Phosphate uptake was determined in fixed samples in preference to unfixed live samples (Moutin *et al*., 2002) to decrease the uncertainties associated with the disruption of live cells deposited on filters (Kiene and Linn, 1999). Fixation of phosphate uptake samples allowed direct comparison with the phosphate uptake of flow sorted cells. The limitation of fixation is that some of the accumulated phosphate could leak out of fixed cells after the cell membranes become compromised. However, we believe the advantages gained, including good reproducibility (e.g. Supplementary online Fig. S3) for both phosphate rate measurements and cell sorting results, outweigh the uncertainties caused by possible phosphate loss from fixed cells.

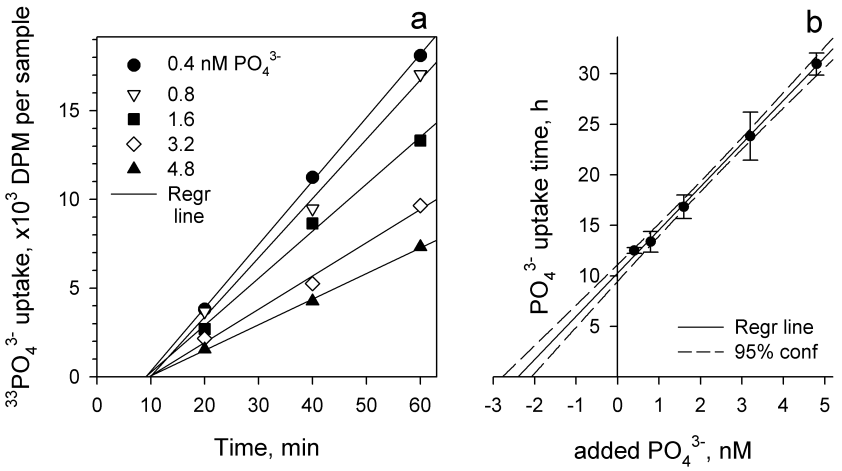

Fig. 6. Typical bioassay estimation of maximum ambient phosphate concentrations and uptake rates from the cruise in September 2005.
a. Time series at different phosphate (PO_4^{3-}) concentrations with corresponding regression lines (Regr line). Phosphate uptake was estimated in a dilution series, in which [^{33}P]orthophosphate at 0.02 nM was diluted with different amounts of non-labelled phosphate.
b. The relationships between added phosphate concentration and phosphate uptake time. Error bars show single standard errors. The *y*-axis intercept of the regression line in plot (b) is an estimate of uptake time (10 h) at maximum ambient phosphate concentration, which is the *x*-axis intercept (2.4 nM). See details in the text.

The sampled particulate material was harvested onto 0.2 μm polycarbonate filters (Poretics Corporation, USA), autoclaved in a solution of 0.5 M LiCl and 1 mM phosphate (LiCl–PO_4 buffer), adjusted to pH 9 (Grillo and Gibson, 1979) and washed with two 5-ml aliquots of the same buffer. Radioactivity retained on the filters was measured as disintegrations per minute (DPM) using a liquid scintillation counter (Tri-Carb 3100, Perkin Elmer, USA). The rate of phosphate uptake was calculated as the slope of the linear regression of radioactivity against incubation time (e.g. Fig. 6a) and then used to calculate phosphate uptake time by dividing the amount of radioactivity added to a sample by the rate of its uptake per hour. The resulting uptake times were plotted against a corresponding concentration of added phosphate and extrapolated using linear regression (Fig. 6b). The slope of the regression line gives an estimate of phosphate uptake rate. The ordinate intercept of the regression line gives an estimate of phosphate uptake time of the sum of the ambient concentration plus the transport constant (Wright and Hobbie, 1966). The transport constant is a measure of the affinity of the microbial uptake system for phosphate; the lower the constant the more effective the uptake at low phosphate concentration. Considering that bacterioplankton should be well adapted to living at ambient nanomolar phosphate concentrations, we assumed that their transport constant would be negligibly small compared with ambient phosphate concentrations and hence report here maximum ambient concentrations that should be treated as upper estimates.

Flow cytometric sorting of radioactively labelled microbial cells

Phosphate uptake by *Pro* and *Syn*, LNA, and all bacterioplankton cells, were determined at 14 stations on the October 2005 cruise. Five replicate 1.6 ml samples were incubated in crystal clear screw cap microtubes (Starlab, Milton Keynes, UK) at *in situ* temperature, in the dark, and then fixed with 1% PFA after 2 h. Phosphate uptake of algal cells was determined at three stations (14.3°N, 26.7°N, 30.9°N). To determine phosphate uptake by algal cells and rare *Syn* additional 100 ml samples were placed into 250-ml acid-washed polycarbonate bottles, spiked with radiolabelled phosphate, and then incubated in the dark and fixed with 1% PFA in the presence of 0.01% pluronic solution (Biegala *et al.*, 2003). In all cases [^{33}P]orthophosphate (> 2500 Ci mmol^{-1}) was added at 80 pM tracer concentration.

Fixed samples were stored at 2°C for microbial flow sorting which was carried out within 48 h. *Pro*, *Syn* and algae were flow cytometrically sorted from unstained samples using their autofluorescence (Supplementary online Fig. S1) and bacterioplankton and LNA cells were flow sorted from SYBR Green I DNA stained samples (Supplementary online Fig. S2). To flow sort rare algal and *Syn* cells (Fig. 3), 100 ml samples fixed with 1% PFA were gently sifted through 0.8 μm pore-size polycarbonate filters to concentrate these cells. Cells were washed off the filter and resuspended in 1.6 ml of unfiltered sample before being flow sorted. Additionally algae were also flow sorted from SYBR Green I DNA stained samples (Zubkov *et al.*, 2007) to check for possible by-sorting of bacterioplankton cells with algal cells from unstained samples. The by-sorting was seen to be insignificant (data not shown). The FACSort was set at single-cell sort mode (the highest sorting purity of the instrument) and the target cells were gated and flow sorted at a rate 1–250 particles s^{-1}. Sorted cells were collected onto 0.2 μm pore size polycarbonate filters autoclaved in LiCl–phosphate buffer and washed twice with the same buffer. Radioactivity retained on filters was measured as DPM using a liquid scintillation counter (Tri-Carb 3100) or as counts per minute (CPM) using an ultra-low level liquid scintillation counter (1220 Quantulus, Wallac, Finland). In the second case of counting samples of low radioactivity, DPM were calculated to correct for the radioactive decay. Three proportional numbers of cells were sorted from 1, 2 and 3×10^3 cells to 20, 40 and 60×10^3 cells (Supplementary online Fig. S3), and the mean cellular phosphate uptake was determined from the slope of the linear regression of radioactivity against the number of sorted bacterial cells.

The activity of the flow sorted microbial groups was determined by multiplying the average radioactivity per cell observed for that group by the abundance of the group. The relative group activity was calculated as the group fraction of the total bacterioplankton community and the microbial uptake rates of phosphate estimated using the bioassays,

corresponded to the total sample. Total microbial uptake was determined in samples used for flow sorting by filtering triplicate subsamples of 40, 80 and 120 μl onto 0.2 μm pore size polycarbonate filters autoclaved in LiCl–phosphate buffer, washed twice with the same buffer and radio-assayed as described above. Total bacterioplankton uptake was calculated by multiplying the activity of an average flow-sorted bacterioplankton cell by the concentration of bacterioplankton in the analysed sample to compare with the total microbial uptake (Fig. 4a). Similarly *Pro*, *Syn*, LNA and algal group uptake was calculated by multiplying the activity of an average flow-sorted cell by the concentration of the respective group in the sample. A sum of the group uptake was compared with the bacterioplankton uptake (Fig. 4b). Hence, we could estimate the flow-sorted group uptake rate of phosphate at ambient concentrations by multiplying the microbial uptake rate by the relative group activity. The cell-specific activity was calculated by dividing the absolute group activity by group abundance.

Sorting purity was assessed routinely by sorting one type of beads from a mixture of two 0.5 μm beads with different yellow-green fluorescence. The sorted material was 99% enriched with the target beads; the sorted bead recovery was > 95%.

Fluorescence in situ *hybridization identification of microbial groups*

The composition of total bacterioplankton was assessed using a set of probes (Table 2) at eight stations (11.7°N, 14.3°N, 17.5°N, 20.7°N, 23.1°N, 26.7°N, 30.9°N, 35.7°N) on the October 2005 cruise. Five replicated 1.6 ml seawater subsamples from the thermos flasks were fixed with 1% PFA at 2°C for 12 h and stored frozen at −80°C. Subsequently, samples were thawed and 0.1–0.4 ml aliquots spotted onto small pieces of 0.2 μm polycarbonate filters. Fluorescence *in situ* hybridization was performed as described previously (Pernthaler *et al*., 2002) with some modifications. These were in brief that cells were embedded in low-gelling point agarose and permeabilized by subsequent treatments with lysozyme for 60 min at 37°C and then achromopeptidase for a further 30 min at 37°C. The filters were then washed in sterile water and 96% (v/v) ethanol for 1 min. Filter sections were submerged in the buffer-probe mix and incubated at 46°C on a rotation shaker for 2 h. The hybridization buffer and probe working solution (50 ng μl^{-1}) were mixed in a ratio of 300:1. This buffer contained varying amounts of formamide, depending on the probe used (Table 2). Washing was carried out at 48°C in 50 ml of prewarmed washing buffer with varying amounts of NaCl, again depending on the probe used. After the washing step, filters were transferred into 15 ml of 1× phosphate buffered saline (PBS) for 15 min at room temperature, to ensure equilibration. Signal amplification was performed using custom made fluorescein (FITC) labelled tyramide (Pernthaler and Amann, 2004) and one part of the tyramide solution was added to 300 parts of amplification buffer for 15 min at 37°C in the dark. The filters were then washed with 1× PBS for 15 min at room temperature followed by subsequent washes in sterile water and 96% ethanol for 1 min. Counter-staining with 4,6-diamidino-2-phenylindole (DAPI; 1 μg ml^{-1}), mounting, and microscopic evaluations were performed as described previously (Pernthaler and Amann, 2004). Cells were counted under a Zeiss Axiovert II motorized epifluorescence microscope (Carl Zeiss, Jena, Germany), equipped with a 100× UV Plan Apochromat objective and excitation/emission filters 360/420 for DAPI and 490/515 for FITC and an automated image analysis system the KS300 (Image Associates, Bicester, UK). At least 300 cells were counted per sample and probe-positive cells were presented as percentages of DAPI stained cells. The FISH data were presented as mean percentages plus/minus a single standard deviation averaged for samples collected at the eight stations.

In addition to FISH analysis of total bacterioplankton at four selected stations (14.3°N, 26.7°N, 30.9°N, 35.7°N) the LNA and *Pro* cells were flow sorted using a sterilized FACSCalibur flow cytometer (BD, Oxford, UK) with an installed in-line 0.1 μm cartridge filter (Pall corporation, Michigan, USA) following staining with SYBR Green (Supplementary online Fig. S2). Approximately 1×10^5 cells were sorted and subsequently filtered on 0.2-μm pore-size polycarbonate filters for FISH analysis as described above using the SAR11-524 probe (Morris *et al*., 2002) to affiliate the LNA cells and 405Pro, 645HLI and 645HLII probes (West *et al*., 2001) to affiliate the *Pro* cells (Table 2). The FISH data for flow sorted samples were presented as mean percentages plus/minus a single standard deviation averaged for the four analysed stations.

Acknowledgements

We gratefully acknowledge the captains, officers and crew aboard the R.R.S. James Clark Ross and R.R.S. Discovery and the R.V. Maria S. Merian for their help during the four cruises. We acknowledge Katie Chamberlain for her help with inorganic nutrient analyses. We thank Michael Sleigh, Raymond Leakey and Adrian Martin for their critical comments on earlier drafts of the article. We thank three anonymous reviewers for constructive criticism of an earlier version of this article. This study was supported by the UK Natural Environment Research Council (NERC) through the Atlantic Meridional Transect (AMT) consortium (NER/O/S/2001/00680), the National Oceanography Centre and Plymouth Marine Laboratory Core Programmes. This is contribution number 138 of the AMT program. It also forms part of the NERC Marine Microbial Metagenomics consortium (NE/C50800X/1). The research cruise on the RV Maria S. Merian was funded by the Max Planck Society, the German Research Foundation and the German Federal Ministry of Education and Research. The research of M.V.Z. was supported by an advanced research fellowship from the NERC (NER/I/S/2000/01426).

References

Amann, R.I., Krumholz, L., and Stahl, D.A. (1990) Fluorescent-oligonucleotide probing of whole cells for determinative, phylogenetic, and environmental studies in microbiology. *J Bacteriol* **172:** 762–770.

Ammerman, J.W., Hood, R.R., Case, D.A., and Cotner, J.B. (2003) Phosphorus deficiency in the Atlantic: an emerging paradigm in oceanography. *EOS* **84:** 165–170.

Arrigo, K.R. (2005) Marine microorganisms and global nutrient cycles. *Nature* **437:** 349–355.

Bertilsson, S., Berglund, O., Karl, D.M., and Chisholm, S.W. (2003) Elemental composition of marine *Prochlorococcus* and *Synechococcus*: implications for the ecological stoichiometry of the sea. *Limnol Oceanogr* **48:** 1721–1731.

Biegala, I.C., Not, F., Vaulot, D., and Simon, N. (2003) Quantitative assessment of picoeukaryotes in the natural environment by using taxon-specific oligonucleotide probes in association with tyramide signal amplification-fluorescence *in situ* hybridization and flow cytometry. *Appl Environ Microbiol* **69:** 5519–5529.

Daims, H., Bruhl, A., Amann, R., Schleifer, K.H., and Wagner, M. (1999) The domain-specific probe EUB338 is insufficient for the detection of all Bacteria: development and evaluation of a more comprehensive probe set. *Syst Appl Microbiol* **22:** 434–444.

Ferguson, R.L., and Sunda, W.G. (1984) Utilization of amino-acids by planktonic marine bacteria – importance of clean technique and low substrate additions. *Limnol Oceanogr* **29:** 258–274.

Giovannoni, S.J., Tripp, H.J., Givan, S., Podar, M., Vergin, K.L., Baptista, D., *et al.* (2005) Genome streamlining in a cosmopolitan oceanic bacterium. *Science* **309:** 1242–1245.

Grillo, J.F., and Gibson, J. (1979) Regulation of phosphate accumulation in the unicellular cyanobacterium *Synechococcus*. *J Bacteriol* **140:** 508–517.

Gundersen, K., Heldal, M., Norland, S., Purdie, D.A., and Knap, A.H. (2002) Elemental C, N, and P cell content of individual bacteria collected at the Bermuda Atlantic Time-Series Study (BATS) site. *Limnol Oceanogr* **47:** 1525–1530.

Heldal, M., Scanlan, D.J., Norland, S., Thingstad, F., and Mann, N.H. (2003) Elemental composition of single cells of various strains of marine *Prochlorococcus* and *Synechococcus* using X-ray microanalysis. *Limnol Oceanogr* **48:** 1732–1743.

Ho, T.Y., Quigg, A., Finkel, Z.V., Milligan, A.J., Wyman, K., Falkowski, P.G., and Morel, F.M.M. (2003) The elemental composition of some marine phytoplankton. *J Phycol* **39:** 1145–1159.

Johnson, Z.I., Zinser, E.R., Coe, A., McNulty, N.P., Woodward, E.M.S., and Chisholm, S.W. (2006) Niche partitioning among *Prochlorococcus* ecotypes along ocean-scale environmental gradients. *Science* **311:** 1737–1740.

Karl, D., Letelier, R., Tupas, L., Dore, J., Christian, J., and Hebel, D. (1997) The role of nitrogen fixation in biogeochemical cycling in the subtropical North Pacific Ocean. *Nature* **388:** 533–538.

Karner, M.B., DeLong, E.F., and Karl, D.M. (2001) Archaeal dominance in the mesopelagic zone of the Pacific Ocean. *Nature* **409:** 507–510.

Kiene, R.P., and Linn, L.J. (1999) Filter-type and sample handling affect determination of organic substrate uptake by bacterioplankton. *Aquat Microb Ecol* **17:** 311–321.

Li, W.K.W. (1994) Primary production of prochlorophytes, cyanobacteria, and eukaryotic ultraphytoplankton – measurements from flow cytometric sorting. *Limnol Oceanogr* **39:** 169–175.

Lipschultz, F. (1995) Nitrogen-specific uptake rates of marine phytoplankton isolated from natural populations of particles by flow cytometry. *Mar Ecol Prog Ser* **123:** 245–258.

Marie, D., Partensky, F., Jacquet, S., and Vaulot, D. (1997) Enumeration and cell cycle analysis of natural populations of marine picoplankton by flow cytometry using the nucleic acid stain SYBR Green I. *Appl Environ Microbiol* **63:** 186–193.

Martiny, A.C., Coleman, M.L., and Chisholm, S.W. (2006) Phosphate acquisition genes in *Prochlorococcus* ecotypes: evidence for genome-wide adaptation. *Proc Natl Acad Sci USA* **103:** 12552–12557.

Mary, I., Heywood, J.L., Fuchs, B.M., Amann, R., Tarran, G.A., Burkill, P.H., and Zubkov, M.V. (2006) SAR11 dominance among metabolically active low nucleic acid bacterioplankton in surface waters along an Atlantic Meridional Transect. *Aquat Microb Ecol* **45:** 107113.

Mills, M.M., Ridame, C., Davey, M., La Roche, J., and Geider, R.J. (2004) Iron and phosphorus co-limit nitrogen fixation in the eastern tropical North Atlantic. *Nature* **429:** 292–294.

Moore, L.R., Ostrowski, M., Scanlan, D.J., Feren, K., and Sweetsir, T. (2005) Ecotypic variation in phosphorus acquisition mechanisms within marine picocyanobacteria. *Aquat Microb Ecol* **39:** 257–269.

Morris, R.M., Rappe, M.S., Connon, S.A., Vergin, K.L., Siebold, W.A., Carlson, C.A., and Giovannoni, S.J. (2002) SAR11 clade dominates ocean surface bacterioplankton communities. *Nature* **420:** 806–810.

Moutin, T., Thingstad, T.F., Van Wambeke, F., Marie, D., Slawyk, G., Raimbault, P., and Claustre, H. (2002) Does competition for nanomolar phosphate supply explain the predominance of the cyanobacterium *Synechococcus*? *Limnol Oceanogr* **47:** 1562–1567.

Olson, R.J., Zettler, E.R., and DuRand, M.D. (1993) Phytoplankton analysis using flow cytometry. In *Handbook of Methods in Aquatic Microbial Ecology.* Kemp, P.F., Sherr, B.F., Sherr, E.B., and Cole, J.J. (eds). Boca Raton, FL, USA: Lewis, pp. 175–186.

Pernthaler, A., and Amann, R. (2004) Simultaneous fluorescence *in situ* hybridization of mRNA and rRNA in environmental bacteria. *Appl Environ Microbiol* **70:** 5426–5433.

Pernthaler, A., Pernthaler, J., and Amann, R. (2002) Fluorescence *in situ* hybridization and catalyzed reporter deposition for the identification of marine bacteria. *Appl Environ Microbiol* **68:** 3094–3101.

Sanudo-Wilhelmy, S.A., Kustka, A.B., Gobler, C.J., Hutchins, D.A., Yang, M., Lwiza, K., *et al.* (2001) Phosphorus limitation of nitrogen fixation by *Trichodesmium* in the central Atlantic Ocean. *Nature* **411:** 66–69.

Schönhuber, W., Zarda, B., Eix, S., Rippka, R., Herdman, M., Ludwig, W., and Amann, R. (1999) *In situ* identification of cyanobacteria with horseradish peroxidase-labeled, rRNA-targeted oligonucleotide probes. *Appl Environ Microbiol* **65:** 1259–1267.

Thingstad, T.F., Krom, M.D., Mantoura, R.F.C., Flaten, G.A. F., Groom, S., Herut, B., *et al.* (2005) Nature of phosphorus limitation in the ultraoligotrophic eastern Mediterranean. *Science* **309:** 1068–1071.

Van Mooy, B.A.S., Rocap, G., Fredricks, H.F., Evans, C.T., and Devol, A.H. (2006) Sulfolipids dramatically decrease phosphorus demand by picocyanobacteria in oligotrophic marine environments. *PNAS* **103:** 8607–8612.

West, N., and Scanlan, D. (1999) Niche-partitioning of *Prochlorococcus* populations in a stratified water column in

the eastern North Atlantic Ocean. *Appl Environ Microbiol* **65:** 2585–2591.
West, N.J., Schönhuber, W.A., Fuller, N.J., Amann, R.I., Rippka, R., Post, A.F., and Scanlan, D.J. (2001) Closely related *Prochlorococcus* genotypes show remarkably different depth distributions in two oceanic regions as revealed by *in situ* hybridization using 16S rRNA-targeted oligonucleotides. *Microbiology* **147:** 1731–1744.
Woodward, E.M.S. (1994) *Nutrient Analysis Techniques.* Plymouth, UK: Plymouth Marine Laboratory.
Woodward, E.M.S. (2002) Nanomolar detection of phosphate and nitrate using liquid waveguard technology. *EOS* **83:** 92.
Wright, R.T., and Hobbie, J.E. (1966) Use of glucose and acetate by bacteria and algae in aqautic ecosystems. *Ecology* **47:** 447–464.
Wu, J.F., Sunda, W., Boyle, E.A., and Karl, D.M. (2000) Phosphate depletion in the western North Atlantic Ocean. *Science* **289:** 759–762.
Zubkov, M.V., and Burkill, P.H. (2006) Syringe pumped high speed flow cytometry of oceanic phytoplankton. *Cytometry A* **69:** 1010–1019.
Zubkov, M.V., and Tarran, G.A. (2005) Amino acid uptake of *Prochlorococcus* spp. in surface waters across the South Atlantic Subtropical Front. *Aquat Microb Ecol* **40:** 241–249.
Zubkov, M.V., Sleigh, M.A., Burkill, P.H., and Leakey, R.J.G. (2000) Picoplankton community structure on the Atlantic Meridional Transect: a comparison between seasons. *Prog Oceanogr* **45:** 369–386.
Zubkov, M.V., Tarran, G.A., and Fuchs, B.M. (2004) Depth related amino acid uptake by *Prochlorococcus* cyanobacteria in the Southern Atlantic tropical gyre. *FEMS Microbiol Ecol* **50:** 153–161.
Zubkov, M.V., Burkill, P.H., and Topping, J.N. (2007) Flow cytometric enumeration of DNA-stained oceanic planktonic protists. *J Plankton Res* **29:** 79–86.
Zwirglmaier, K., Heywood, J.L., Chamberlain, K., Woodward, E.M.S., Zubkov, M.V., and Scanlan, D.J. (2007) Basin-scale distribution patterns of picocyanobacterial lineages in the Atlantic Ocean. *Environ Microbiol* **9:** 1278–1290.

Supplementary material

The following supplementary material is available for this article online:

Fig. S1. Characteristic flow cytometric signatures of flow sorted picophytoplanktonic groups.

Fig. S2. Characteristic flow cytometric signatures of DNA stained and flow sorted groups of bacterioplankton.

Fig. S3. An example of the flow sorting radioassay.

This material is available as part of the online article from http://www.blackwell-synergy.com

